Formation of Nascent Secretory Vesicles from the *trans*-Golgi Network of Endocrine Cells Is Inhibited by Tyrosine Kinase and Phosphatase Inhibitors

Cary D. Austin* and Dennis Shields*‡

*Developmental and Molecular Biology and ‡Anatomy and Structural Biology, Albert Einstein College of Medicine, Bronx, New York 10461

Abstract. Recent evidence suggests that secretory vesicle formation from the TGN is regulated by cytosolic signaling pathways involving small GTP-binding proteins, heterotrimeric G proteins, inositol phospholipid metabolism, and protein serine/threonine phosphorylation. At the cell surface, protein phosphorylation and dephosphorylation on tyrosine residues can rapidly modulate cytosolic signaling pathways in response to extracellular stimuli and have been implicated in the internalization and sorting of signaling receptors. To determine if phosphotyrosine metabolism might also regulate secretory vesicle budding from the TGN, we treated permeabilized rat pituitary GH_3 cells with inhibitors of either tyrosine phosphatases or tyrosine kinases. We demonstrate that the tyrosine phosphatase inhibitors pervanadate and zinc potently inhibited budding of nascent secretory vesicles. Tyrphostin A25 (TA25) and other tyrosine kinase inhibitors also prevented secretory vesicle release, suggesting that vesicle formation requires both phosphatase and kinase activities. A stimulatory peptide derived from the NH_2 terminus of the small GTP-binding protein ADP ribosylation factor 1 (ARF1) antagonized the inhibitory effect of TA25, indicating that both agents influence the same pathway leading to secretory vesicle formation. Anti-phosphotyrosine immunoblotting revealed that protein tyrosine phosphorylation was enhanced after treatment with tyrosine phosphatase or kinase inhibitors. Subcellular fractionation identified several tyrosine phosphorylated polypeptides of ~175, ~130, and 90–110 kD that were enriched in TGN-containing Golgi fractions and tightly membrane associated. The phosphorylation of these polypeptides correlated with inhibition of vesicle budding. Our results suggest that in endocrine cells, protein tyrosine phosphorylation and dephosphorylation are required for secretory vesicle release from the TGN.

Vesicular transport through the eukaryotic secretory pathway is a highly regulated process that requires spatial and temporal specificity (for reviews see references 4, 19, 51). Members of the Rab family of Ras-related small GTP-binding proteins appear to provide temporal specificity in vesicle release, docking, and fusion (for reviews see references 41, 44). Other small GTP-binding proteins, ADP ribosylation factors (ARFs)[1], also play a critical regulatory role in vesicular transport. ARF proteins are required in several steps of membrane traffic and have been shown to regulate assembly of vesicle coat proteins and maintain organelle integrity (for reviews see 5, 15). In addition, ARF can activate phospholipase D (10, 12, 31, 32), a phenomenon that may play a central role in the regulation of membrane traffic through the metabolism of inositol phospholipids (for reviews see 14, 38). Enzymes in inositol phospholipid metabolism directly implicated in membrane trafficking in both yeast and mammalian cells include phosphatidylinositol transfer protein (23, 24, 43) and phosphatidylinositol 3-kinase (for reviews see 14, 38, 54). Heterotrimeric GTP-binding proteins (G proteins) have also been implicated in the regulation of membrane traffic (for reviews see 6, 41) and can interact directly with ARF (13, 50). These observations raise the possibility that membrane trafficking events may be regulated by an interconnected network of cytosolic signaling pathways reminiscent of those initiated by cell surface signaling receptors.

In polypeptide hormone–producing cells, the packaging of proteins into nascent secretory vesicles occurs in the TGN, a major site of protein sorting in the endomembrane

Address all correspondence to Dennis Shields, Department of Developmental and Molecular Biology, Albert Einstein College of Medicine, 1300 Morris Park Avenue, Bronx, NY 10461. Tel.: (718) 430-3306 Fax: (718) 430-8567. E-mail: shields@aecom.yu.edu

1. *Abbreviations used in this paper*: ARF, ADP ribosylation factor; GH, growth hormone; Lav A, lavendustin A; PLD, phospholipase D; Prl, prolactin; proSRIF, prosomatostatin; PVDF, polyvinyl difluoride; TA1, tyrphostin A1; TA25, Tyrphostin A25; TNBS, trinitrobenzene sulfonate.

© The Rockefeller University Press, 0021-9525/96/12/1471/13 $2.00

system. We are investigating the requirements for both formation of secretory vesicles from the TGN and prohormone processing in endocrine cells and have used permeabilized cells (1, 11, 37, 62) derived from growth hormone (GH)– and prolactin (Prl)–secreting pituitary GH_3 cells stably expressing human prosomatostatin (proSRIF) (16). Recent studies from our laboratory and others suggest that the regulation of secretory vesicle release from the TGN is complex, involving ARF1 (11), rabs 6 and 8 (26, 30), heterotrimeric G proteins (35, 45, and Austin, C.D., Y.-G. Chen, and D. Shields, unpublished observations), metabolism of inositol phospholipids (43), and protein serine/threonine phosphorylation (30, 40, 42, 46, 63). It is unclear, however, how the packaging of vesicle cargo proteins in the TGN lumen could be linked to such an intricate network of cytosolic regulation during coat assembly and budding of secretory vesicles. One way this might be achieved is by protein tyrosine phosphorylation. Protein tyrosine phosphorylation is a reversible, dynamic process that plays an essential role in fundamental cellular processes such as growth and differentiation. Receptor tyrosine kinases transduce signals across the plasma membrane to regulate several cytosolic signaling pathways involving the activities of nonreceptor tyrosine kinases and phosphatases, small GTP-binding proteins such as Ras, serine/threonine kinases, and enzymes involved in inositol phospholipid metabolism such as phosphatidylinositol 3-kinase and phospholipases C and D (for review see 60). Phosphotyrosine metabolism has also been implicated in signaling events involving heterotrimeric G proteins (36, 39, 55, 61). Although phosphotyrosine metabolism is believed to participate mainly in signal transduction pathways initiated at the cell surface, recent evidence suggests that it may also transduce signals arising intracellularly from membrane-enclosed organelles (for review see 2). Nascent secretory vesicle formation in endocrine cells presents an attractive target for such regulation since regulated secretion itself is signal mediated. Here we have used protein tyrosine phosphatase and kinase inhibitors to examine the role of phosphotyrosine metabolism in the release of nascent secretory vesicles from the TGN of permeabilized cells. Our data implicate both tyrosine phosphatase and kinase activities in secretory vesicle formation through a signaling pathway involving the vesicle coat assembly factor ARF1.

Materials and Methods

Sodium orthovanadate was purchased from Fisher Scientific (Pittsburgh, PA). Tyrphostin A25 (TA25), tyrphostin A1 (TA1), lavendustin A (Lav A), genestein, okadaic acid, staurosporin, and calphostin C were purchased from Calbiochem-Novabiochem Corp. (La Jolla, CA). Picrylsulfonic acid (trinitrobenzene sulfonate [TNBS]) was purchased from Sigma Chemical Co. (St. Louis, MO). The 16–amino acid peptide (GNIFANLFKGLFGKKE) corresponding to the NH_2 terminus of human ARF1 (residues 2–17) was synthesized in the Laboratory for Molecular Analysis (Albert Einstein College of Medicine). Rabbit anti-Prl serum, anti-GH serum, and anti-SRIF-propeptide serum, which recognizes preproSRIF, proSRIF, and the free propeptide (16), were described previously (1). Monoclonal antiphosphotyrosine antibody (PY20) for immunofluorescence microscopy and horseradish peroxidase–conjugated recombinant antiphosphotyrosine antibody (HRPO-RC20) for immunoblotting were purchased from Transduction Laboratories (Lexington, KY). Rabbit anti-TGN38 serum was generously provided by Sharon Milgram (University of North Carolina, Chapel Hill, NC) and Richard Mains (Johns Hopkins University, Baltimore, MD). Rabbit anti-DNP serum was described previously (22). Cy3™-conjugated goat anti–rabbit IgG and FITC-conjugated goat anti–mouse IgG antibodies were purchased from Jackson ImmunoResearch Laboratories, Inc. (West Grove, PA). Rat anterior pituitary GH_3 cells stably expressing human preproSRIF (GH_3.Hu.S) were described previously (16).

Preparation of Pervanadate

10 mM sodium orthovanadate was freshly prepared and treated with 10 mM H_2O_2 for 10 min at room temperature just before use. Residual H_2O_2 was removed by incubating for 5 min at room temperature with 100 μg/ml (21,000 U/mg) catalase (18, 49). For mock incubations, orthovanadate was omitted.

Cell Culture and Pulse Labeling

GH_3.Hu.S cells were grown and pulse labeled as previously described (1, 56) with 500 μCi [^{35}S]methionine/ml, which in the case of proSRIF radiolabels only the amino-terminal propeptide region, and chased in the presence of complete growth medium for 2 h at 19°C. These conditions result in retention of most of the radiolabeled hormones in the TGN (62). Cells were then placed at 4°C before subsequent treatment.

Cell Surface Labeling

Intact cells were surface labeled either before or after the 2-h 19°C chase as described previously (22). Briefly, cultures were chilled at 4°C, washed three times in PBS-T (125 mM NaCl, 25 mM $NaPO_4$, pH 8.0), and then incubated in 10 mM TNBS in PBS-T at 4°C for 15 min. Cells were then washed three times in PBS-T and once in PBS-T containing 1 mg/ml BSA before subsequent treatment.

Permeabilized Cell Preparation and In Vitro Incubations

Preparation of permeabilized cells by a swell–scrape method was described previously (1, 62). The control incubation condition for these experiments contained ~5×10^5 permeabilized cells, 20 mM Hepes, pH 7.3, 125 mM KCl, 2.5 mM $MgCl_2$, 1 mM ATP, 200 μM GTP, 10 mM creatinine phosphate, 160 μg/ml creatinine phosphate kinase (ATP-regenerating system), 0.5 mM PMSF, and 5 μg/ml trasylol. Incubation for 2 h at 37°C under these conditions is sufficient to reconstitute both proSRIF processing and nascent secretory vesicle release from the TGN (62). Permeabilized cells were pretreated with or without the indicated concentration of inhibitors for 10 min at 4°C before addition of the ATP-regenerating system and incubation at 37°C. The final concentration of DMSO in the reactions did not exceed 0.5%, which itself had no effect on proSRIF processing or vesicle budding.

Immunoprecipitation and Densitometry

The assay for nascent secretory vesicle budding was based on quantitating the release of radiolabeled hormones into a 15,000 *g* supernatant after an in vitro incubation (1, 11, 37, 62). Processing of radiolabeled proSRIF was determined by quantitating the percentage of anti-SRIF-propeptide generated from proSRIF after immunoprecipitation using the anti-SRIF propeptide antibody (16). After the incubation, permeabilized cells were pelleted and lysed in detergent and the lysates and supernatants containing nascent secretory vesicles were treated sequentially with anti-Prl, anti-GH, and anti-SRIF propeptide serum as described previously (1, 56). Immunoreactive material was resolved by SDS-PAGE and detected by fluorography. Band intensities were quantitated using a computing densitometer (model 300A; Molecular Dynamics, Sunnyvale, CA) and Image Quant 3.3 software (Molecular Dynamics).

Immunoblotting

Proteins were precipitated from detergent lysates at −20°C by adding 9 vol acetone/0.1 N HCl and from 15,000 *g* supernatants or sucrose gradient fractions at 4°C by adding an equal volume of ice cold 20% (wt/vol) TCA. The precipitates were dissolved in SDS gel buffer by low-power microprobe sonication, resolved by SDS-PAGE, and transferred to polyvinyl difluoride (PVDF) membranes. Membranes were subsequently probed

for tyrosine-phosphorylated proteins with HRPO-RC20 antibody (1:2,500 dilution), or for TGN38 or the TNP moiety with appropriate antiserum (1:100 dilution) followed by horseradish peroxidase–conjugated anti–rabbit IgG (secondary antibody, 1:1,000 dilution), and detected by chemiluminescence (Amersham Corp., Buckinghamshire, England).

Subcellular Fractionation

To isolate an enriched TGN/Golgi membrane fraction after treatment of ~1 × 10^7 permeabilized GH_3.Hu.S cells with pervanadate, cells were homogenized using eight strokes of a stainless steel ball-bearing homogenizer (12.7-μm clearance) in 1.5 ml homogenization buffer (0.25 M sucrose, 20 mM Hepes KOH, pH 7.3, 2.5 mM $MgCl_2$, 0.5 mM PMSF, 5 μg/ml trasylol, and 100 μM pervanadate). The homogenate was adjusted to ~1.4 M sucrose and loaded onto a step gradient comprising 2 ml 2 M sucrose cushion overlaid with ~2 ml adjusted homogenate ("load zone"), 7 ml 1.2 M sucrose, and 2 ml 0.8 M sucrose; all solutions contained 20 mM Hepes KOH, pH 7.3, 2.5 mM $MgCl_2$, and 100 μM pervanadate. The gradient was centrifuged for ~14 h at 35,000 rpm at 4°C in a rotor (model SW41Ti; Beckman Instrs., Fullerton, CA) to float the TGN/Golgi membranes to equilibrium (between 1.2 M and 0.8 M sucrose, 62). Fractions (1 ml each) were collected from the top of the gradient and fraction aliquots were assayed for total protein by the method of Bradford (8), radiolabeled hormones by immunoprecipitation (see above), and TGN38, tyrosine-phosphorylated proteins, and the TNP moiety by immunoblotting (see above). It was previously shown that most of the pulse-labeled GH and proSRIF-derived peptides from intact cell homogenates following a 2-h ~19°C chase cofractionated with the distal TGN/Golgi marker enzymes galactosyl and sialyl transferases and the TGN marker protein TGN-38 near the top of the gradient (fractions 2–4), whereas most of the total protein and >95% of the endoplasmic reticulum marker ribophorin I remained in the load zone (62).

Immunofluorescence Microscopy

After appropriate treatments, permeabilized cells were sedimented briefly at 15,000 *g*, resuspendend in fixative (4% paraformaldehyde), and then sedimented onto poly-L-lysine–coated glass slides. Samples were permeabilized with 0.2% saponin in 100 mM NaCl, 10 mM Tris, pH 7.4, containing 1% FCS and 0.5% BSA as blocking agents. Samples were then incubated in the presence of anti-TGN38 serum (1:100 dilution) with or without 1:100 PY20 antiphosphotyrosine antibody (1:100 dilution), followed by incubation with Cy3™-conjugated goat anti–rabbit IgG antibody (1:300 dilution) and FITC-conjugated goat anti–mouse IgG antibody (1:100 dilution). Slides were examined using a laser scanning confocal microscope (model MRC 600; BioRad Labs, Hercules, CA) using identical settings. Images were processed using Adobe Photoshop™ software using identical settings except where indicated.

Results

Tyrosine Phosphatase and Kinase Inhibitors Prevent Nascent Secretory Vesicle Release from the TGN

To determine if phosphotyrosine metabolism was required for nascent secretory vesicle release from the TGN, permeabilized cells were incubated with tyrosine phosphatase or tyrosine kinase inhibitors. As observed previously (1, 11, 37, 62), secretory vesicles containing TGN-derived radiolabeled Prl, GH, and proSRIF-derived peptides were efficiently released into the 15,000 *g* supernatant in control incubations (Fig. 1, lanes *1* and *2*). In the presence of the tyrosine phosphatase inhibitors pervanadate or zinc (21, 47, 61), vesicle release was completely inhibited (Fig. 1, lanes *3–6*). The tyrosine phosphatase inhibitor sodium orthovanadate also prevented budding of nascent secretory vesicles (data not shown). Consistent with earlier observations (42), inhibitors of serine/threonine phosphatases (up to 5 μM okadaic acid or 5 mM sodium fluoride) had no effect on vesicle budding efficiency (data not shown). Based on the preceding data, we anticipated that inhibition of tyrosine phosphorylation might stimulate vesicle release. However TA25, a tyrosine kinase inhibitor that competes with the tyrosine substrate (20, 34), completely inhibited release of nascent secretory vesicles (Fig. 1, lanes *7* and *8*). Lav A and genestein, tyrosine kinase inhibitors that compete with ATP (34), also prevented vesicle budding, although somewhat less effectively (Fig. 1, lanes *9* and *10*, and data not shown), most likely because vesicle budding reactions contained 1 mM ATP. In contrast, vesicle budding was not inhibited by up to 150 nM calphostin C (data not shown), a specific inhibitor of protein kinase C. Staurosporin, a less selective protein kinase inhibitor, also had no significant effect on vesicle release (up to 2.5 μM, data not shown), a result consistent with previous observations (42). These data suggested that both phosphorylation and dephosphorylation of tyrosine residues, but not serine or threonine residues, were required for release of nascent secretory vesicles from the TGN. In contrast to vesicle budding, proSRIF processing, which was ~30% efficient in control incubations, was unaffected by inhibitors of phosphotyrosine metabolism (Fig. 1, *bottom panel*, lanes *1–10*).

The dose response of secretory vesicle release to the tyrosine phosphatase inhibitor pervanadate (EC_{50} ~10 μM; Fig. 2, ■) was similar to that observed for inhibition of tyrosine dephosphorylation in several systems (18, 25, 47, 49). To ensure that vesicle budding was not inhibited by the H_2O_2 used to generate the pervanadate ion, mock incubations containing equivalent amounts of catalase-treated H_2O_2 were performed. As expected, there was no

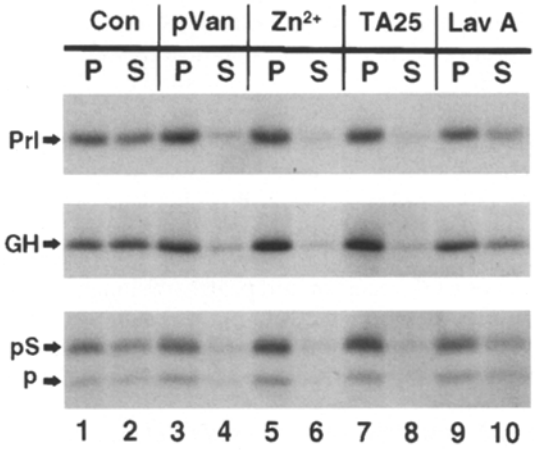

Figure 1. Tyrosine phosphatase and kinase inhibitors prevent nascent secretory vesicle release but not proSRIF processing in permeabilized cells. Pulse-chased permeabilized cells (Materials and Methods) were preincubated for 10 min at 4°C without inhibitors (lanes *1* and *2*) or with 50 μM pervanadate (lanes *3* and *4*), 25 μM zinc chloride (lanes *5* and *6*), 100 μM TA25 (lanes *7* and *8*), or 100 μM LavA (lanes *9* and *10*), followed by further incubation for 2 h at 37°C with ATP and GTP. Samples were subsequently separated into pellet (*P*, lanes *1*, *3*, *5*, *7*, and *9*) and nascent vesicle–containing supernatant (*S*, lanes *2*, *4*, *6*, *8*, and *10*) fractions by centrifugation at 15,000 *g* for 10 s and sequential immunoprecipitations performed with rabbit antisera to Prl, GH, and SRIF-propeptide. The immunoreactive peptides were resolved by SDS-PAGE and detected by fluorography. *pS*, proSRIF; *p*, SRIF propeptide.

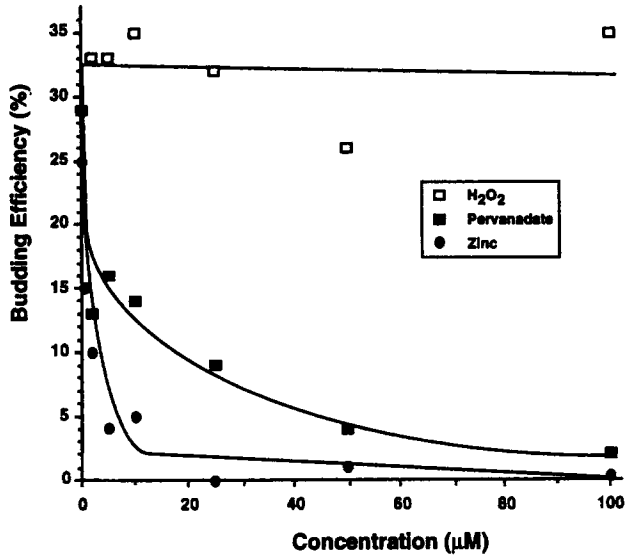

Figure 2. Dose response of nascent secretory vesicle release to tyrosine phosphatase inhibitors. Permeabilized cells were preincubated for 10 min at 4°C with the indicated concentrations of catalase-treated pervanadate (■), H_2O_2 alone (□) (Materials and Methods), or zinc chloride (●) followed by further incubation for 2 h at 37°C with ATP and GTP. Nascent secretory vesicle formation was determined by immunoprecipitation using anti-GH serum followed by densitometric quantitation of the fluorograms. The values represent averages from two similar experiments. Comparable results were obtained using anti-Prl and anti-SRIF propeptide serum.

inhibitory effect (Fig 2, □). Sodium orthovanadate, a less potent tyrosine phosphatase inhibitor (18, 53, 59), prevented secretory vesicle release at significantly higher concentrations (EC_{50} ~250 μM; data not shown). Tyrosine phosphatases exhibit differential sensitivity to zinc, making it a useful diagnostic reagent (61). Zinc was a slightly more effective inhibitor of nascent vesicle release than pervanadate (EC_{50} ~2 μM; Fig. 2, ●). The dose response of vesicle budding to the tyrosine kinase inhibitor TA25 (EC_{50} ~10 μM; Fig. 3 *A*, ■) was similar to that observed for inhibition of EGF receptor and $p210^{Bcr\text{-}Abl}$ kinase activity (34). In contrast, equivalent amounts of the inactive structural analogue tyrphostin A1 (TA1)(20) had no inhibitory effect (Fig. 3 *A*, □).

Inhibition of Nascent Secretory Vesicle Release by TA25 Is Antagonized by the NH_2 Terminus of ARF1

Recent studies from our laboratory have implicated ARF1 and in particular, its amino-terminal peptide (residues 2–17), in stimulating the release of nascent secretory vesicles from the TGN (11). As observed previously, secretory vesicle release in the absence of TA25 was stimulated approximately twofold by 25 μM ARF1 peptide (Fig. 3 *B*). To determine if ARF1 and tyrosine phosphorylation regulate vesicle budding through a common pathway, permeabilized cells were incubated in the presence of both the ARF1 peptide and TA25 simultaneously. We reasoned that if a shared pathway were involved, the dose response to TA25 might be altered by the presence of the ARF1 peptide. If, however, the two agents influenced vesicle

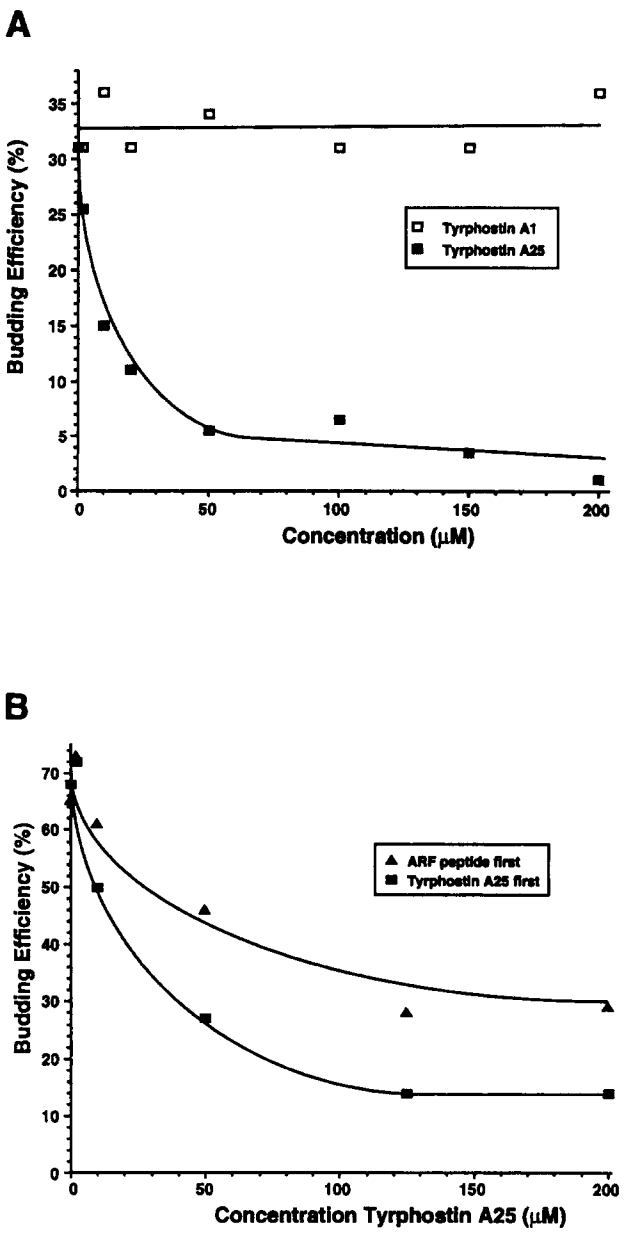

Figure 3. Dose response of nascent secretory vesicle release to tyrosine kinase inhibitors. (*A*) Tyrphostin A25 and its inactive structural analogue tyrphostin A1. Permeabilized cells were preincubated for 10 min at 4°C with the indicated concentrations of TA25 (■) or TA1 (□) followed by further incubation for 2 h at 37°C with ATP and GTP. (*B*) The ARF1 NH_2-terminal peptide (residues 2–17) antagonizes inhibition of nascent secretory vesicle budding by tyrphostin A25. Permeabilized cells were first preincubated for 10 min at 4°C with the indicated concentrations of TA25 followed by addition of 25 μM ARF peptide for an additional 10 min at 4°C (■). Alternatively, cells were first preincubated for 10 min at 4°C with 25 μM ARF1 peptide followed by addition of the indicated concentrations of TA25 for an additional 10 min at 4°C (▲). Samples were subsequently incubated for 2 h at 37°C with ATP and GTP. Nascent secretory vesicle formation was determined by immunoprecipitation using anti-Prl serum. The values represent averages from two similar experiments. Comparable results were obtained using anti-GH and anti-SRIF propeptide serum.

budding by distinct mechanisms, the ARF1 peptide would fail to modify the dose response to TA25. Consistent with the first hypothesis, the ARF1 peptide antagonized the inhibitory effect of TA25, raising the EC_{50} three- to fourfold (compare Fig. 3 *A*, ■ with 3 *B*, ■ and ▲). Most significantly, when permeabilized cells were preincubated with the ARF1 peptide before addition of TA25 (Fig. 3 *B*, ▲), the antagonism was more pronounced than when pretreatment with TA25 preceded ARF1 (Fig. 3 *B*, ■), reinforcing the idea that ARF1 peptide antagonized inhibition by TA25.

Tyrosine Phosphatase and Kinase Inhibitors Increase Protein Tyrosine Phosphorylation While Inhibiting Nascent Vesicle Budding

We reasoned that since the above pharmacological perturbations inhibited nascent secretory vesicle release, it should be possible to identify specific changes in protein tyrosine phosphorylation that correlated with inhibition of vesicle budding. After incubation of permeabilized cells with the tyrosine phosphatase and kinase inhibitors, antiphosphotyrosine immunoblotting was performed. Protein tyrosine phosphorylation was minimal when vesicle release was prevented by low temperature (Fig. 4 *A*, lanes *1* and *2*) and in control incubations under budding conditions (Fig. 4 *A*, lanes *3* and *4*). In contrast, incubation with 50 μM pervanadate caused marked tyrosine phosphorylation relative to control incubations in both cell pellet and 15,000 *g* supernatant fractions (Fig. 4 *A*, compare lanes *5* and *6* to lanes *3* and *4*). Treatment with 50 μM zinc, which appeared to be more selective than pervanadate, also resulted in protein tyrosine phosphorylation predominantly in the pellet fraction (Fig. 4 *A*, lane *7*). Paradoxically, limited protein tyrosine phosphorylation was also observed in pellet fractions in the presence of tyrosine kinase inhibitors (Fig. 4 *A*, compare lanes lanes *9*, *11*, and *13* with lane *3*). The most conspicuously enhanced band in samples treated with 50 μM TA25, 100 μM Lav A, or 200 μM genestein was a phosphoprotein of ~130 kD (e.g., Fig. 4 *A*, compare lanes *13* and *3*, *lower arrowhead*), although the tyrosine phosphorylation of other polypeptides (e.g., ~175 kD and 90–110 kD) was also increased. These results raised the possibility that inhibitors of tyrosine phosphatases and kinases prevented nascent secretory vesicle release by permitting increased tyrosine phosphorylation of one or more polypeptides, possibly those of ~175, ~130, and 90–110 kD.

To further test the correlation between protein tyrosine phosphorylation and regulation of vesicle budding, the inhibitor dose response of tyrosine phosphorylation was examined. In agreement with the zinc-mediated inhibition of vesicle release (Fig. 2, ●), enhanced protein tyrosine phosphorylation in pellet fractions required low micromolar levels of zinc (Fig. 4 *B*, lanes *5–7*). However, in samples incubated with pervanadate, tyrosine-phosphorylated proteins appeared at lower concentrations (Fig. 4 *B*, lanes *2–4*), although maximal tyrosine phosphorylation occurred at pervanadate levels close to those needed to inhibit vesicle release (Fig. 2, ■). Enhanced tyrosine phosphorylation also occurred at low micromolar levels of the tyrosine kinase inhibitor TA25 (Fig. 4 *C*, lanes *1–5*) but not TA1 (data not shown), in agreement with the dose response for inhibition of vesicle budding (Fig. 3 *A*, ■). Remarkably, pretreatment with the NH_2-terminal ARF1 peptide significantly reduced the low level of tyrosine phosphorylation observed in control incubations (Fig. 4 *C*, compare lane *6* with lane *1*) as well as that induced by TA25 (Fig. 4 *C*, compare lanes *7–10* with lanes *2–5*), results consistent with the antagonism observed between ARF1 peptide and TA25 for vesicle budding (Fig. 3 *B*). Antagonism of TA25-induced phosphorylation was particularly evident for polypeptides of ~175 and ~130 kD (Fig. 4 *C*, *arrowheads*) and somewhat less for other polypeptides including those of 90–110 kD (Fig. 4 *C*, *bracket*).

During our standard 2-h vesicle budding incubation, release of nascent secretory vesicles begins after a 15–20-min lag (62). If enhanced protein tyrosine phosphorylation was indeed responsible for inhibition of vesicle release, phosphorylation would be expected to occur early in the incubation with inhibitors, before vesicle budding. The results in Fig. 5 confirmed this prediction. In the presence of pervanadate, maximal tyrosine phosphorylation occurred within 5 min of incubation at 37°C (Fig. 5 *A*, lanes *3–6*). Similar kinetics were observed in the presence of zinc (Fig. 5 *A*, lanes *8–11*). No appreciable tyrosine phosphorylation occurred in the presence of pervanadate or zinc before shifting the temperature to 37°C during the preincubation step (Fig. 5 *A*, compare lane *1* with lanes *2* and *7*, respectively). In the presence of TA25, maximal tyrosine phosphorylation of several polypeptides, including those of ~175, ~130, and 90–110 kD also occurred within 5 min at 37°C (Fig. 5 *B*, *arrowheads* and *bracket*, lanes *1* and *2*). Other polypeptides, however, such as those of ~30–40 kD (Fig. 5 *B*), became phosphorylated only after prolonged (20–60 min) incubation with TA25 and thus were not correlated with inhibition of vesicle budding. Interestingly, tyrosine phosphorylation diminished at later time points (Fig. 5 *B*, lanes *3–5*) and could be completely abolished after prolonged (2 h) incubations with high (e.g., 200 μM) concentrations of TA25, a phenomenon not observed at lower inhibitor concentrations (data not shown). Thus, TA25 had two kinetically distinguishable effects on protein phosphorylation: (*a*) induction of phosphorylation early in the reaction, and (*b*) dephosphorylation later in the incubation, after completion of events leading to inhibition of vesicle budding.

Tyrosine-phosphorylated Proteins Colocalize with the TGN

We predicted that if phosphotyrosine metabolism were regulating secretory vesicle release from the TGN, then some tyrosine-phosphorylated proteins would be associated with this organelle. To examine this possibility, subcellular fractionation was performed after incubation of permeabilized cells with pervanadate using an equilibrium flotation gradient designed to separate Golgi membranes from total microsomes (3, 62). As previously demonstrated using intact cells (62), most of the radiolabeled Prl, GH, and proSRIF-derived peptides cofractionated with the TGN marker protein TGN-38 near the top of the gradient (Fig. 6, *A* and *B*, fractions *2–4*), whereas the bulk of the total protein remained in the load zone (Fig. 6 *D*, △, fractions *8–11*). This ~17-fold enrichment of radiolabeled

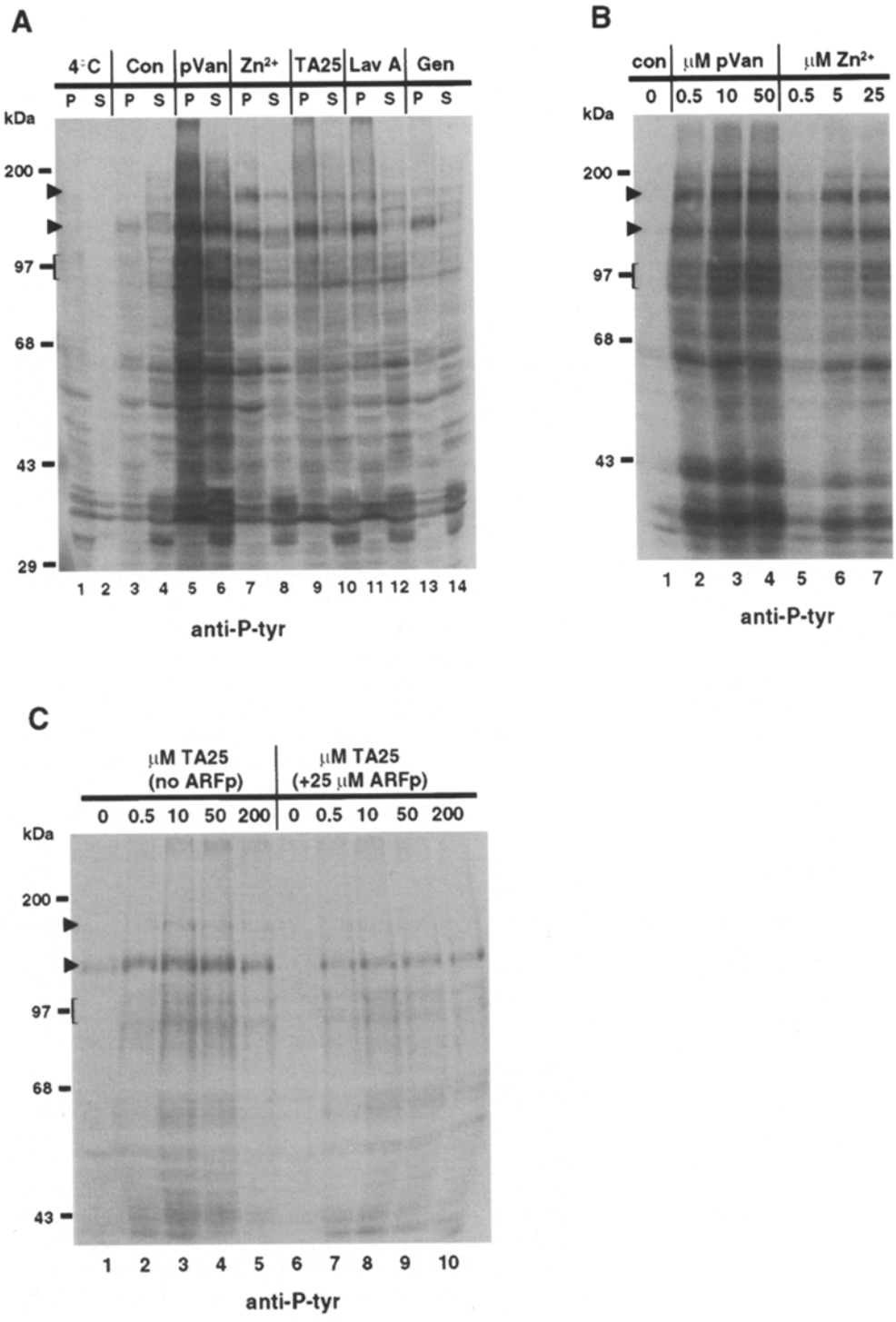

Figure 4. Protein tyrosine phosphorylation after treatment of permeabilized cells with inhibitors of tyrosine phosphatases or kinases. (*A*) Antiphosphotyrosine immunoblot. Permeabilized cells were preincubated for 10 min at 4°C without inhibitors (lanes *1–4*) or with 50 μM pervanadate (lanes *5* and *6*), 50 μM zinc chloride (lanes *7* and *8*), 50 μM TA25 (lanes *9* and *10*), 100 μM Lav A (lanes *11* and *12*), or 200 μM genestein (lanes *13* and *14*) followed by further incubation for 30 min at 37°C with ATP and GTP (lanes *3–14*). Samples were then separated into cell pellet (*P*) and nascent vesicle–containing supernatant (*S*) fractions. (*B*) Dose response to tyrosine phosphatase inhibitors. Permeabilized cells were preincubated with or without (lane *1*) the indicated concentrations of pervanadate (lanes *2–4*) or zinc chloride (lanes *5–7*) followed by incubation for 2 h at 37°C. Cell pellet fractions are shown. (*C*) Dose response to the tyrosine kinase inhibitor TA25 in the presence or absence of the ARF1 NH_2-terminal peptide. Permeabilized cells were preincubated for 10 min at 4°C without (lanes *1–5*) or with 25 μM ARF1 peptide (lanes *6–10*) followed by addition of the indicated concentrations of TA25 and preincubation for an additional 10 min at 4°C. Samples were subsequently incubated for 2 h at 37°C with ATP and GTP. Cell pellet fractions are shown. In each experiment, the total protein was resolved by SDS-PAGE, transferred to PVDF membranes, and analyzed by antiphosphotyrosine immunoblotting (Materials and Methods). *Upper arrowhead*, ~175-kD polypeptide; *lower arrowhead*, ~130-kD polypeptide; *bracket*, 90–110-kD polypeptides.

hormones per mg protein in fractions 2–4 relative to the load zone indicated that the subcellular distribution was maintained after in vitro incubation with pervanadate, consistent with the inability of secretory vesicle cargo to exit the TGN when vesicle budding was blocked. Most significantly, antiphosphotyrosine immunoblotting of the gradient fractions revealed that the ~175-, ~130-, and 90–110-kD phosphorylated proteins were also enriched (~14-fold per mg protein) in fractions 2–4 relative to the load zone (Fig. 6 *C*, *arrowheads* and *bracket*). In contrast, other ma-

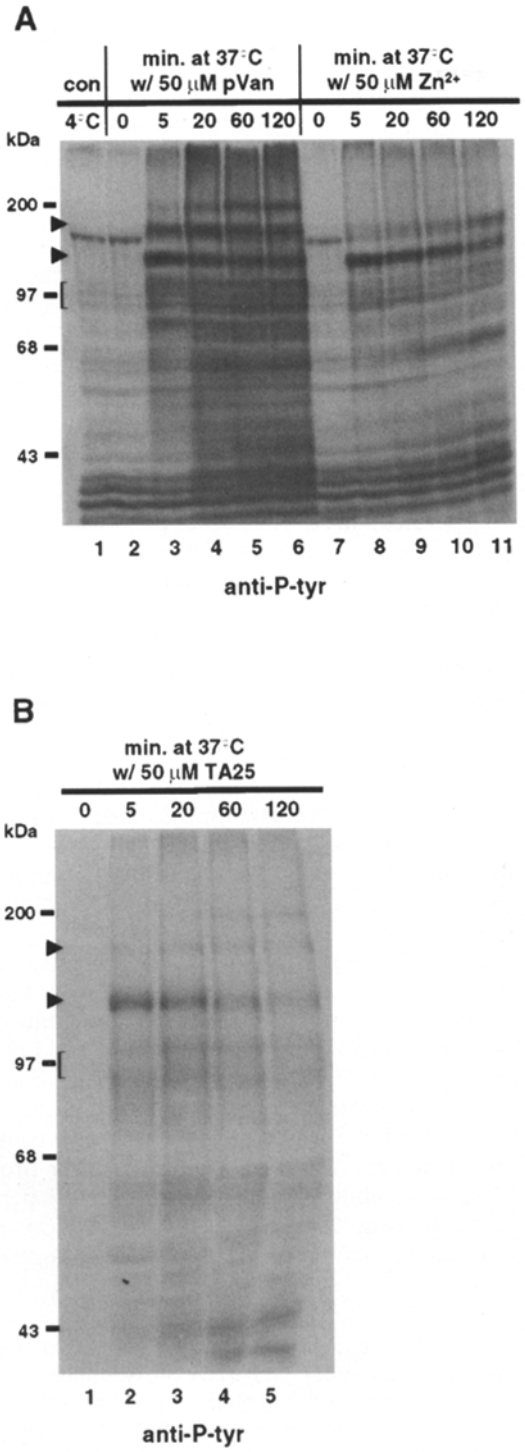

Figure 5. Enhanced protein tyrosine phosphorylation occurs early in incubations with inhibitors of tyrosine phosphatases or kinases. (*A*) Kinetics of tyrosine phosphorylation after treatment with tyrosine phosphatase inhibitors. Permeabilized cells were preincubated without (lane *1*) or with 50 μM pervanadate (lanes *2–6*) or 50 μM zinc chloride (lanes *7–11*) followed by incubation with ATP and GTP for the indicated times at 37°C (lanes *2–11*). Cell pellet fractions are shown. (*B*) Kinetics of tyrosine phosphorylation after treatment with tyrosine kinase inhibitors. Permeabilized cells were preincubated with 50 μM TA25 followed by incubation for the indicated times at 37°C with ATP and GTP (lanes *2–5*). Cell pellet fractions are shown. Samples were analyzed by antiphosphotyrosine immunoblotting. *Upper arrowhead*, ~175-kD polypeptide; *lower arrowhead*, ~130-kD polypeptide; *bracket*, 90–110-kD polypeptides.

jor tyrosine-phosphorylated proteins, e.g., 30–40-kD polypeptides, remained near the bottom of the gradient (Fig. 6 *C*, fractions *9–13*).

The cell surface is a well-known site of protein tyrosine phosphorylation (60). To test the possibility that the high–molecular weight tyrosine-phosphorylated proteins in gradient fractions 2–4 reflected contamination with plasma membrane, we also examined the gradient distribution of total cell surface protein. Before permeabilization, intact cells were exposed to TNBS, which results in the covalent attachment of TNP moieties to externally exposed proteins (22 and references within). Total plasma membrane proteins could then be monitored on immunoblots using anti-DNP antiserum. The anti-DNP signal consisted of multiple bands and was very specific (>15-fold increase in signal after TNBS labeling, data not shown). When intact cells were labeled with TNBS just before cell permeabilization and incubation with pervanadate, the anti-DNP signal remained almost entirely near the bottom of the gradient and cofractionated with the bulk of the total protein (Fig. 6 *D*, ■, fractions *8–11*). This suggested that the tyrosine phosphorylated proteins in fractions 2–4 were not derived from en masse plasma membrane contamination. It might be argued, however, that these high–molecular weight tyrosine-phosphorylated proteins were derived from the temporal pool of membrane protein exposed at the cell surface before the 19°C chase and had subsequently changed subcellular distribution during the 19°C chase. To examine this possibility, intact cells were labeled with TNBS before the 19°C chase. After cell permeabilization and incubation with pervanadate, the anti-DNP signal again remained almost entirely near the bottom of the gradient (Fig. 6 *D*, ●, fractions *8–11*). These results demonstrated that the tyrosine-phosphorylated proteins found to cofractionate with TGN membranes in fractions 2–4 were not due to bulk plasma membrane contamination produced by the 19°C chase. Selective contamination by individual cell surface proteins that comprise a very small percentage of total cell surface protein, however, cannot be excluded.

To confirm that tyrosine-phosphorylated polypeptides were localized to the TGN, we performed double-label indirect immunofluorescence using the antiphosphotyrosine antibody together with anti-TGN38 serum. Although the cells had been permeabilized and incubated under a variety of conditions, the TGN38-immunoreactive material displayed a perinuclear staining pattern characteristic of the TGN and Golgi apparatus (Fig. 7, *left*, Fig. 8). Significant FITC-staining of cell nuclei was observed in all samples (Fig. 7, *middle*), even in the absence of antiphosphotyrosine antibody (Fig. 7 *A*, *middle*) resulting from nonspecific binding of FITC-conjugated secondary antibody. We predicted that after pervanadate treatment of permeabilized cells, antiphosphotyrosine-specific staining would increase in the cytoplasmic region of the cells, including the TGN. In agreement with our immunoblotting data (Fig. 6 *C*), pervanadate treatment enhanced phosphoty-

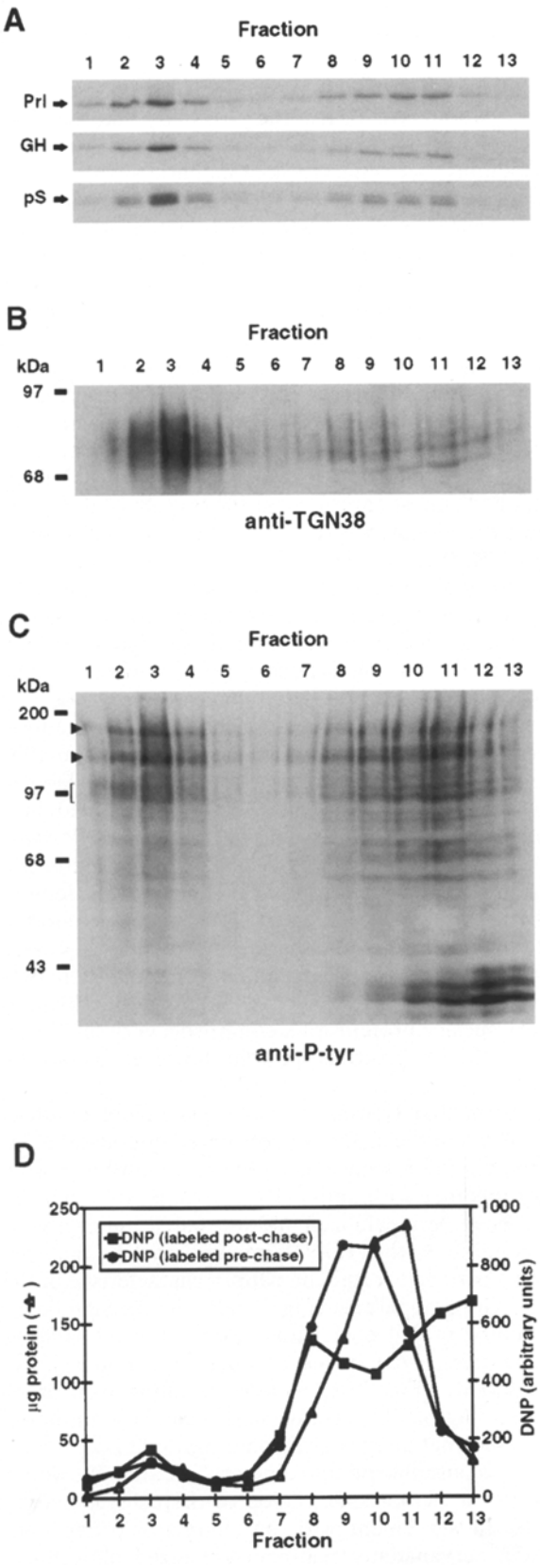

Figure 6. High–molecular weight tyrosine-phosphorylated proteins cofractionate with TGN markers. Permeabilized cells were preincubated with 100 μM pervanadate followed by incubation for 30 min at 37°C with ATP and GTP. The permeabilized cells were homogenized and the homogenate fractionated on an equilibrium flotation gradient designed to separate the TGN/Golgi apparatus from total microsomes (Materials and Methods). (*A*) An aliquot from each fraction was sequentially immunoprecipitated with antisera to Prl, GH, and SRIF-propeptide (*pS*) followed by SDS-PAGE and fluorography. (*B*) An aliquot of each fraction was transferred to PVDF membrane and immunoblotted with anti-TGN38 antiserum. Mature, polysialylated TGN38 appears as a smeared doublet at ~85 kD (30). (*C*) An aliquot of each fraction was transferred to PVDF membrane and immunoblotted with antiphosphotyrosine antibody. *Upper arrowhead*, ~175-kD polypeptide; *lower arrowhead*, ~130-kD polypeptide; *bracket*, 90–110-kD polypeptides. (*D*) Distribution of total protein (△). In separate experiments, intact cells were surface labeled with TNBS either before(●) or after (■) incubation at 19°C (Materials and Methods), permeabilized, and preincubated with 100 μM pervanadate followed by incubation for 30 min at 37°C with ATP and GTP. Cell homogenates were fractionated and aliquots analyzed by anti-DNP immunoblotting and densitometry.

rosine staining of the TGN (Fig. 7 *D*, *arrows* and *right*). Zinc or TA25 treatment resulted in less cytoplasmic staining, but with preserved TGN colocalization (Fig. 7, *E* and *F*, *arrows* and *right*). No FITC staining was observed in the cytoplasmic region after incubation in the absence of inhibitors at either 4°C (Fig. 7 *B*, *middle*) or under budding-permissive conditions at 37°C (Fig. 7 *C*, *middle*), indicating that in inhibitor-treated samples, cytoplasmic staining was phosphotyrosine specific. Moreover, pretreatment of the phosphotyrosine antibody with either phosphotyrosine or phenyl phosphate abolished this staining (data not shown). This data provided further evidence that inhibitor treatment enhanced protein tyrosine phosphorylation at the TGN while inhibiting secretory vesicle release.

Membrane Association of Tyrosine-phosphorylated Proteins

Incubation of permeabilized cells with pervanadate resulted in appearance of significant amounts of tyrosine-phosphorylated proteins in the low-speed (15,000 *g*) supernatant as well as in the pellet fraction (Fig. 4 *A*, lanes *6* and *5*, respectively), an effect not observed with the other inhibitors. Tyrosine-phosphorylated proteins appeared in the low-speed supernatant primarily between 5 and 20 min of incubation with pervanadate at 37°C (data not shown). Because these vesicle-release assays were performed under conditions in which exogenous cytosol was not required (62), the phosphorylated proteins appearing in the low-speed supernatant must have been membrane-associated before incubation at 37°C. It was possible that these proteins were loosely associated with membranes and solubilized during incubation at 37°C. Alternatively, these proteins could have been components of nascent vesicles that did not contain radiolabeled hormones. It is unlikely that this phenomenon represented nonspecific fragmentation of the TGN/Golgi because pervanadate treatment did not result in appearance of TGN lumenal contents (radiolabeled hormones) in the low-speed supernatant fraction (Fig.1, lane *4*). To further exclude this possibility, we compared the morphological localization of the marker protein TGN-38 in permeabilized cells before and after pervanadate treatment (Fig. 8). The overall distribution of TGN-38 was unchanged (compare Fig. 8, *A* and *B*), suggest-

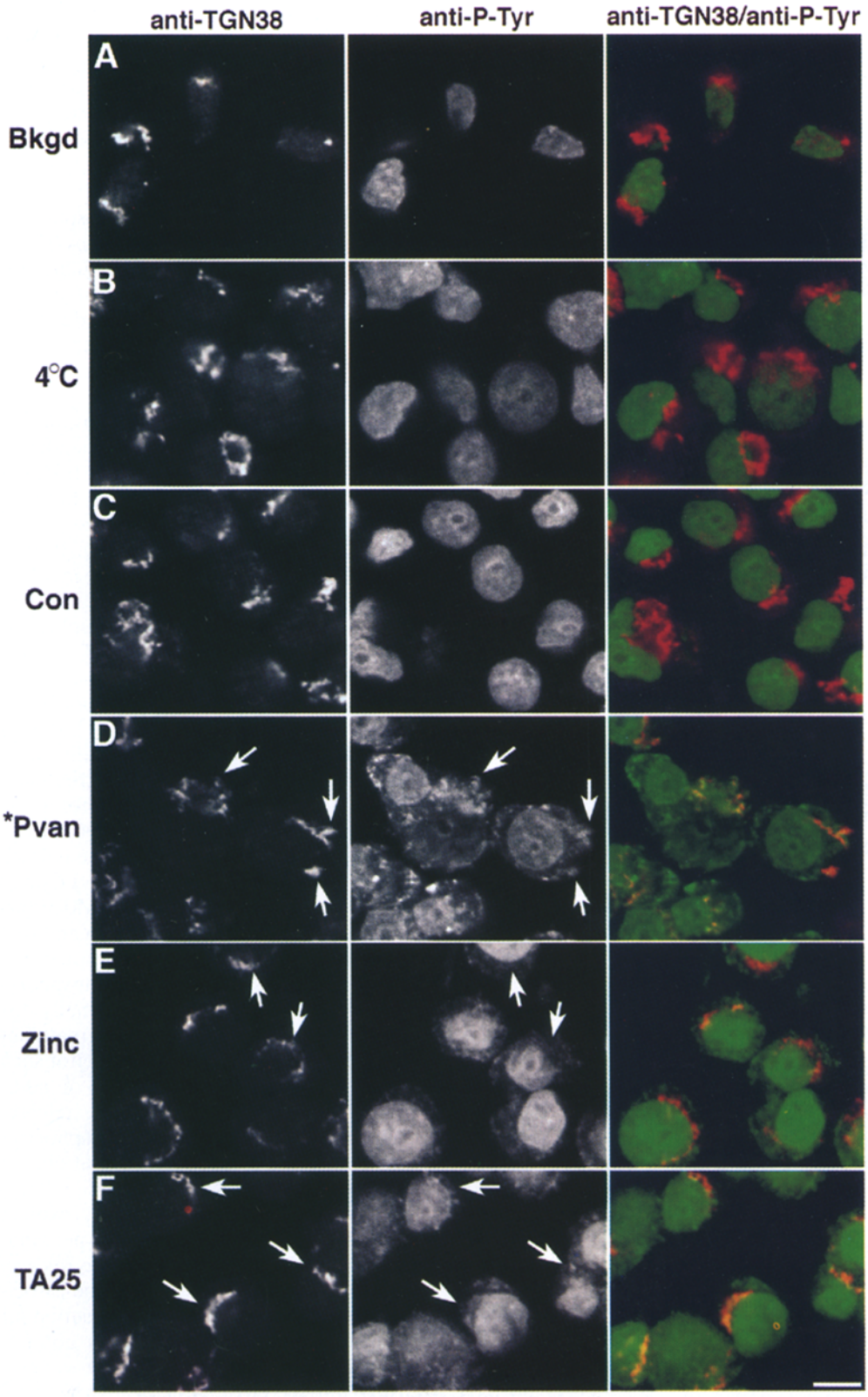

Figure 7. Immunocolocalization of tyrosine-phosphorylated proteins with the TGN in permeabilized cells treated with inhibitors. Permeabilized cells were preincubated at 4°C for 10 min without (*A–C*) or with 50 μM pervanadate (*D*), 50 μM zinc chloride (*E*), or 50 μM TA25 (*F*), followed by incubation at 37°C for 10 min with ATP and GTP (*C–F*). Cells were subsequently fixed and analyzed by double-staining indirect immunofluorescence confocal microscopy (Materials and Methods) using anti-TGN38 primary antiserum with Cy3™-conjugated secondary antibody (*left*) and antiphosphotyrosine primary antibody with FITC-conjugated secondary antibody (*middle*). To determine background FITC staining, antiphosphotyrosine primary antibody was omitted from one sample (*A*). To demonstrate overlap of phosphotyrosine and TGN38, the FITC (*green*) and Cy3™ (*red*) images were digitally merged (*right*). Arrows (*left* and *middle* columns) also identify phosphotyrosine colocalization with TGN38. All images were captured identically. The cytoplasmic FITC fluorescence of pervanadate-treated cells (*D*, *middle* and *right*) was higher than the other samples, and therefore a lower gain setting was used during image processing (*) to preserve contrast. Bar, 10 μM.

ing that the integrity of the Golgi apparatus/TGN was maintained after incubation in the presence of pervanadate.

To determine if the high–molecular weight phosphorylated proteins present in the 15,000 *g* supernatant fraction were membrane-associated or soluble, this material was subjected to several extraction conditions followed by high-speed centrifugation (150,000 *g*). Antiphosphotyrosine immunoblot analysis revealed that the tyrosine-phosphorylated proteins could be sedimented at high-speed (Fig. 9, lanes *1* and *2*), indicating that these proteins were indeed membrane associated. When samples were first extracted with high salt (1 M NaCl) or high pH (100 mM Na-carbon-

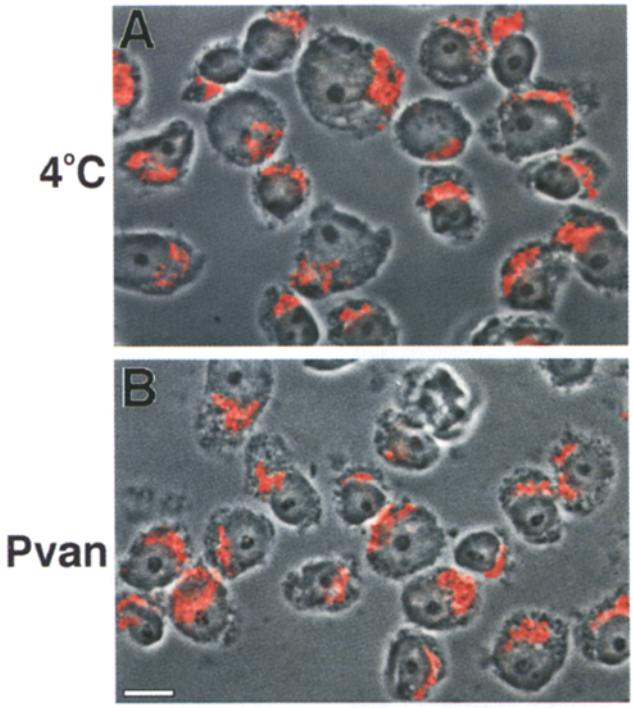

Figure 8. TGN morphology is maintained in permeabilized cells after pervanadate treatment. Permeabilized cells were preincubated at 4°C for 10 min without (*A*) or with (*B*) 50 μM pervanadate followed by incubation at 37°C for 10 min with ATP and GTP (*B*). Cells were analyzed using identical settings by both Normarski optics and indirect immunofluoresence confocal microscopy using anti–TGN-38 antiserum and Cy3™-conjugated secondary antibody (*red*). Identical results were obtained with permeabilized cells incubated in the absence of inhibitors, the presence of 50 μM zinc chloride, or 50 μM TA25 (not shown).

ate, pH 11.5), the ~175-, ~130-, and 90–110-kD phosphoproteins remained in the high-speed pellet fractions whereas the ~30–40-kD phosphoproteins redistributed to the supernatant (Fig. 9, lanes *3–6*). In contrast, upon treatment with the detergent TX-100, the high–molecular weight phosphopolypeptides redistributed to the 150,000 *g* supernatant (Fig. 9, lanes *7* and *8*). These results suggested that the ~175-, ~130-, and 90–110-kD tyrosine phosphorylated proteins were tightly membrane associated and possibly integral membrane proteins. A characteristic feature of many integral membrane proteins is their partitioning into the detergent phase upon TX-114 extraction at 37°C (7). Surprisingly, the high–molecular weight phosphoproteins partitioned into the aqueous phase after TX-114 treatment (Fig. 9, lanes *9–11*). Similar results were obtained in an identical analysis of the tyrosine-phosphorylated proteins from TGN-enriched gradient fractions (data not shown).

Discussion

Nascent Secretory Vesicle Release Requires Both Tyrosine Phosphatase and Kinase Activities

Our results demonstrated that inhibitors of tyrosine phosphatases and kinases prevented release of nascent secretory vesicles from the TGN of permeabilized neuroendocrine cells. Several observations demonstrated that these agents were specific: (*a*) various structurally distinct inhibitors of phosphotyrosine metabolism inhibited secretory vesicle budding (Fig. 1), whereas the tyrosine kinase inhibitor analogue TA1 (Fig. 3 *A*), as well as inhibitors of phosphoserine/threonine metabolism (data not shown), had no effect; (*b*) effective concentrations of each inhibitor (Figs. 2 and 3 *A*) induced changes in the tyrosine phosphorylation status of proteins (Fig. 4) early in the incubations (Fig. 5) and were similar to concentrations reported for inhibition of tyrosine phosphatases and kinases in other systems (18, 25, 34, 47, 49); (*c*) pretreatment with ARF1 peptide antagonized the inhibitory and phosphorylation-enhancing effects of the tyrosine kinase inhibitor TA25 (Figs. 3 *B* and 4 *C*, respectively); (*d*) tyrosine-phosphorylated proteins immunolocalized with the TGN (Fig. 7); (*e*) phosphoproteins implicated in vesicle budding were tightly membrane associated (Fig. 9) and highly enriched in Golgi fractions containing TGN marker proteins (Fig. 6); and (*f*) both the gross morphological appearance of the TGN (Fig. 8) and processing of proSRIF were unaffected (Fig. 1). Protein tyrosine dephosphorylation has been shown to be involved in regulated exocytosis (for example see 27). To our knowledge however, this is the first report implicating phosphotyrosine metabolism in secretory vesicle formation.

Treatment with tyrosine phosphatase inhibitors led to rapid protein tyrosine phosphorylation (Fig. 5 *A*) and revealed that tyrosine kinases were active under these conditions. The somewhat surprising observation that treatment with tyrosine kinase inhibitors also led to rapid protein tyrosine phosphorylation demonstrated that at least one tyrosine kinase was resistant to these inhibitors (see below). Measurements of the dose response (Fig. 4, *B* and *C*) and kinetics (Fig. 5, *A* and *B*) of phosphorylation provided further correlation between tyrosine phosporylation and regulation of vesicle budding. A potential complication of the immunoblotting experiments is that proteins phosphorylated on tyrosine often contain multiple, functionally distinct phosphorylation sites (60). Consequently, treatment with a broad-spectrum tyrosine phosphatase inhibitor such as pervanadate may enhance phosphorylation of additional sites as well as those relevant to vesicle release. Consistent with this idea, maximal tyrosine phosphorylation achieved with pervanadate exceeded that of zinc, a narrow-spectrum tyrosine phosphatase inhibitor (61). Phosphorylation of functionally irrelevant sites may explain why significant phosphorylation was observed at pervanadate concentrations insufficient to prevent vesicle release. Indeed, significant amounts of vesicle membrane-associated phosphoprotein were released after incubation of permeabilized cells with pervanadate; this was not observed with other inhibitors (Fig. 4 *A*). These vesicles could have been nascent secretory vesicles in which the hormone cargo was not packaged. Thus, the possibility remains that pervanadate or any of the other phosphotyrosine metabolism inhibitors interfered with filling of vesicles (i.e., hormone sorting) rather than budding per se. Alternatively, these vesicles could be nonsecretory TGN-derived vesicles, or derived from membranes other than the TGN.

The ~175-, ~130-, and 90–110-kD Tyrosine-phosphorylated Proteins Are Putative Regulators of Secretory Vesicle Formation

The observation that the ~175-, ~130-, and 90–110-kD phosphoproteins were enriched in TGN-containing subcellular fractions implicated these polypeptides in secretory vesicle budding. Tyrosine phosphorylation of these polypeptides correlated with inhibition of vesicle budding with respect to inhibitor dose response and kinetics (Fig. 4). After treatment with various tyrosine kinase inhibitors, tyrosine phosphorylation was particularly evident for the ~130-kD polypeptide and less so for the ~175- and 90–110-kD polypeptides. Furthermore, ARF1 peptide antagonism of tyrosine phosphorylation was most evident for the ~130- and ~175-kD polypeptides (Fig. 4 *C*). These data provide correlative evidence that tyrosine phosphorylation of one or more of these polypeptides inhibit vesicle budding. However, direct proof that the ~175-, ~130-, and 90–110-kD phosphoproteins regulate vesicle formation will require their purification and reconstitution in a highly purified vesicle budding system.

The tyrosine-phosphorylated proteins that cofractionated with the TGN were tightly membrane associated and required detergent treatment for removal (Fig. 9). It is unlikely, therefore, that these proteins were adventitiously associated with Golgi membranes. A characteristic of many integral membrane proteins is their detergent-phase partitioning in the detergent TX-114 upon warming to 37°C (7). Surprisingly, the high–molecular weight phosphoproteins partitioned with the aqueous phase after TX-114 phase separation, suggesting that these proteins were either very tightly membrane-associated peripheral proteins or integral membrane proteins with substantial hydrophilicity that precluded efficient partitioning into the TX-114 detergent phase (48).

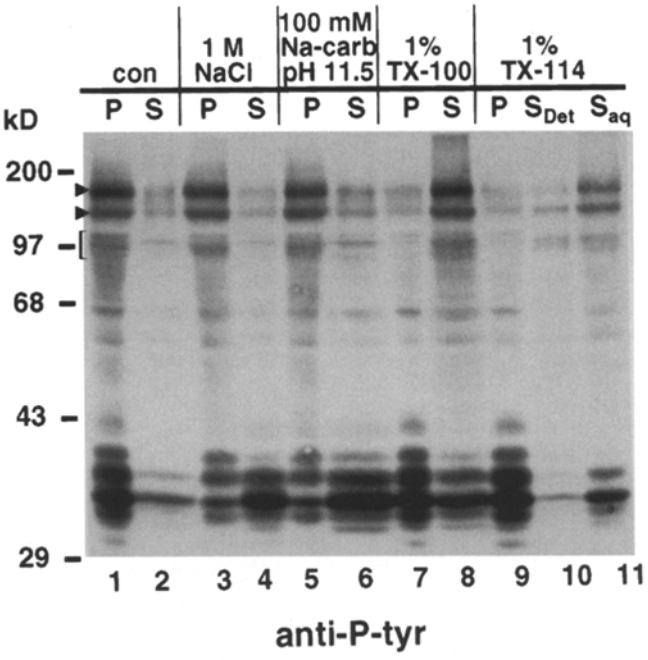

Figure 9. High–molecular weight tyrosine-phosphorylated proteins are tightly membrane associated. Approximately 10^7 permeabilized cells were treated with 100 μM pervanadate for 30 min and centrifuged at 15,000 *g* for 10 s. Supernatant aliquots were incubated for 30 min at 4°C under the following conditions: no extraction (lanes *1* and *2*), 1 M NaCl (lanes *3* and *4*), 100 mM Na_2CO_3, pH 11.5 (lanes *5* and *6*), 1% Triton X-100 (lanes *7* and *8*), and 1% Triton X-114 (lanes *9–11*). Samples were then centrifuged at 150,000 *g* for 20 min to generate pellet (*P*) and high-speed supernatant (*S*) fractions. The Triton X-114 detergent phase (lane *10*) was separated from the aqueous phase (lane *11*) of the high-speed supernatant by incubating 3 min at 37°C and then centrifuging at room temperature for 3 min at 800 *g* through a 6% sucrose cushion (7). All fractions were analyzed by antiphosphotyrosine immunoblotting (Materials and Methods). *Upper arrowhead*, ~175-kD polypeptide; *lower arrowhead*, ~130-kD polypeptide; *bracket*, 90–110-kD polypeptides.

Antagonism between Tyrphostin A25 and ARF1 Peptide

Our results also suggested that both TA25 and the NH_2-terminal ARF1 peptide affected the same pathway leading to secretory vesicle release. Pretreatment with the ARF1 peptide not only shifted the TA25 dose response curve to the right but also reduced basal and TA25-induced tyrosine phosphorylation. It is difficult to integrate these results into a model in which ARF1 serves simply as a structural constituent of vesicle coats. However, recent studies revealing that ARF1 activates phospholipase D (PLD) (10, 12, 31, 32) and interacts directly with heterotrimeric G proteins (5, 13, 50) suggest that ARF1 may regulate intracellular membrane trafficking events through a novel signal transduction pathway. In fact, recent evidence from our laboratory suggests that ARF1 stimulates nascent secretory vesicle release through activation of PLD (Chen et al., manuscript submitted for publication). Interestingly, tyrosine phosphorylation has also been implicated in the regulation of PLD activity (9, 28, 29).

A Model For Regulation of Secretory Vesicle Budding by Phosphotyrosine Metabolism

It might be argued that the observation that vesicle release was prevented by inhibitors of both tyrosine phosphatases and kinases is contradictory. However, cooperation between tyrosine phosphatases and kinases is well documented (for reviews see 17, 57, 58, 60). For example, members of the Src tyrosine kinase family can be activated by tyrosine dephosphorylation of their negative regulatory sites by the receptor tyrosine phosphatases CD45 and PTPα (17). CD45 phosphatase activity is required for T lymphocyte antigen receptor-induced tyrosine phosphorylation, phosphatidylinositol turnover, and Ca^{2+} release from intracellular stores (58). In addition, the widely expressed nonreceptor tyrosine phosphatase SH-PTP2 (or SYP) associates via its SH2 domains with several activated receptor tyrosine kinases, leading to stimulation of phosphatase activity (57, 58). SH-PTP2 does not dephosphorylate the activated receptors, but is instead a positive signaling transducer; SH-PTP2 phosphatase activity is required for receptor tyrosine kinase–mediated responses, possibly via Src-family kinases (17, 57, 58). Tyrosine phosphatases that serve as negative transducers of signaling can also cooperate with specific tyrosine phosphorylation events. In hematopoietic cells for instance, SH-PTP1 (HCP) termi-

nates receptor-mediated signaling. But SH-PTP1 is similarly activated upon binding to tyrosine-phosphorylated molecules via its SH2 domain. Likewise, while our results suggested that secretory vesicle release required cooperation between a tyrosine phosphatase and kinase, they do not preclude the possibility that additional antagonistic phosphatase–kinase relationships also exist.

To explain our observations, we propose a model (Fig. 10) in which the net level of tyrosine phosphate in the target substrate (e.g., the ~130-kD polypeptide, p130) is determined by the balance of tyrosine phosphatase (PTPase) and inhibitor-resistant kinase (PTK_R) activities. Direct inhibition of PTPase activity by pervanadate or zinc disrupts this balance, resulting in enhanced p130 phosphorylation and inhibition of secretory vesicle formation. Treatment with tyrosine kinase inhibitors (e.g., TA25) has a similar consequence early in the budding reaction by indirectly inhibiting PTPase activity, while having a slower or lesser effect on the activity of PTK_R. It should be emphasized that this model is a working hypothesis that explains our observations most simply and could apply equally to any or all the phosphotyrosine polypeptides we have identified; validation of this model will require reconstitution experiments using purified components.

At present we can only speculate how phosphotyrosine metabolism might participate in the regulation of secretory vesicle formation. One possibility is that unidentified receptor tyrosine kinases and/or phosphatases on the TGN membrane transduce signals from the TGN lumen to the cytoplasm in response to interaction with cargo proteins (hormones). At the cell surface, receptor tyrosine kinases and phosphatases bind ligand in a space topologically equivalent to the TGN lumen. Receptor activation leads to recruitment of several effector molecules, which in turn modulate downstream signaling pathways similar to those implicated in secretory vesicle release from the TGN (60). Interestingly, internalization and sorting of activated receptor tyrosine kinases from the plasma membrane to lysosomes requires kinase activity (33; for review see 2). The formation of coated pits on the cell surface appears to be regulated by the activated receptors indirectly, via receptor-mediated signaling pathways (52). It is conceivable that in our system, a tyrosine phosphatase links a stimulated TGN sorting receptor to the activation of ARF and hence to the mobilization of vesicle budding machinery. Further dissection of this pathway using our permeabilized cell system will enable us to address these hypotheses directly.

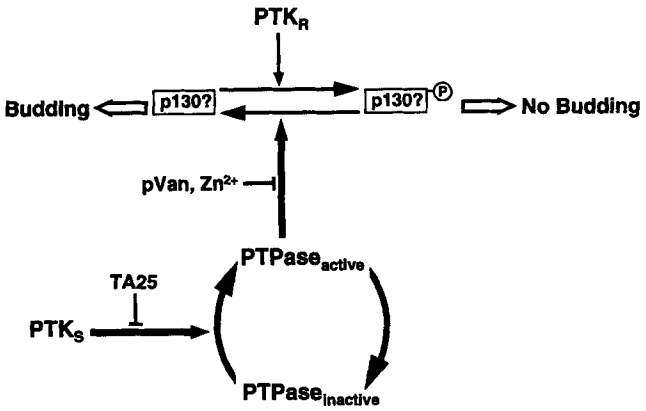

Figure 10. A working model for regulation of secretory vesicle budding by phosphotyrosine metabolism. It is proposed that dephosphorylation of a phosphoprotein (possibly p130) is required for nascent secretory vesicle formation from the TGN. The net level of tyrosine phosphate in p130 is determined by the balance of tyrosine phosphatase ($PTPase_{active}$) and inhibitor-resistant kinase (PTK_R) activities. Direct inhibition of the tyrosine phosphatase with pervanadate (*pVan*) or Zn^{2+} leads to enhanced p130 phosphorylation and inhibition of vesicle budding. Treatment with tyrosine kinase inhibitors such as TA25 has a similar consequence by preventing PTPase activation via a phosphorylation event mediated by an inhibitor-sensitive tyrosine kinase (PTK_S).

We dedicate this paper to Günter Blobel on the occasion of his sixtieth birthday.

We thank Drs. Wai Lam W. Ling, Yeguang Chen, Duncan Wilson, and Tamar Michaeli for helpful suggestions and discussions and Michael Cammer for help with the confocal microscopy experiments.

This work was supported by National Institutes of Health (NIH) grant DK21860 and in part by a grant from the Juvenile Diabetes Foundation to D. Shields. C.D. Austin was supported by a Life and Health Insurance Medical Research Fund M.D.-Ph.D. Scholarship. Core support was provided by an NIH Cancer Center grant P30CA13330.

Received for publication 13 June 1996 and in revised form 9 September 1996.

References

1. Austin, C.D., and D. Shields. 1996. Prosomatostatin processing in permeabilized cells. Calcium is required for prohormone processing but not formation of nascent secretory vesicles. *J. Biol. Chem.* 271:1194–1199.
2. Baass, P.C., G.M. Di Guglielmo, F. Authier, B.I. Posner, and J.J.M. Bergeron. 1995. Compartmentalized signal transduction by receptor tyrosine kinases. *Trends Cell Biol.* 5:465–470.
3. Beckers, C.J.M., D.S. Keller, and W.E. Balch. 1987. Semi-intact cells permeable to macromolecules: use in reconstitution of protein transport from the endoplasmic reticulum to the golgi complex. *Cell.* 50:523–534.
4. Bennett, M.K., and R.H. Scheller. 1993. The molecular machinery for secretion is conserved from yeast to neurons. *Proc. Natl. Acad. Sci. USA.* 90:2559–2563.
5. Boman, A.L., and R.A. Kahn. 1995. Arf proteins: the membrane traffic police. *Trends Biochem. Sci.* 20:147–150.
6. Bomsel, M., and K. Mostov. 1992. Role of heterotrimeric G proteins in membrane traffic. *Mol. Biol. Cell.* 3:1317–1328.
7. Bordier, C. 1981. Phase separation of intergral membrane proteins in Triton X-114 solution. *J. Biol. Chem.* 256:1604–1607.
8. Bradford, M.M. 1976. A rapid and sensitive method for the quantitation of microgram quantities of protein utilizing the principle of protein-dye binding. *Anal. Biochem.* 72:248–254.
9. Briscoe, C.P., A. Martin, M. Cross, and M.J.O. Wakelam. 1995. The roles of multiple pathways in regulating bombesin-stimulated phospholipase D activity in Swiss 3T3 fibroblasts. *Biochem. J.* 306:115–122.
10. Brown, H.A., S. Gutowski, C.R. Moomaw, C. Slaughter, and P.C. Sternweis. 1993. ADP-ribosylation factor, a small GTP-dependent regulatory protein, stimulates phospholipase D activity. *Cell.* 75:1137–1144.
11. Chen, Y.-G., and D. Shields. 1996. ADP-ribosylation factor-1 stimulates formation of nascent secretory vesicles from the trans-Golgi network of endocrine cells. *J. Biol. Chem.* 271:5297–5300.
12. Cockcroft, S., G.M.H. Thomas, A. Fensome, B. Geny, E. Cunningham, I. Gout, I. Hiles, N.F. Totty, O. Truong, and J.J. Hsuan. 1994. Phospholipase D: a downstream effector of ARF in granulocytes. *Science (Wash. DC).* 263:523–526.
13. Colombo, M.I., J. Inglese, C. D'Souza-Schorey, W. Beron, and P.D. Stahl. 1995. Heterotrimeric G proteins interact with the small GTPase ARF. Possibilities for the regulation of vesicular traffic. *J. Biol. Chem.* 270: 24564–24571.
14. De Camilli, P., S.D. Emr, P.S. McPherson, and P. Novick. 1996. Phosphoinositides as regulators in membrane traffic. *Science (Wash. DC).* 271: 1533–1539.
15. Donaldson, J.G., and R.D. Klausner. 1994. ARF: a key regulatory switch in membrane traffic and organelle structure. *Curr. Opin. Cell Biol.* 6:527–532.
16. Elgort, A., and D. Shields. 1994. Prosomatostatin processing in pituitary GH_3 cells. Identification and secretion of the intact propeptide. *J. Biol.*

Chem. 269:30668–30675.
17. Erpel, T., and S.A. Courtneidge. 1996. Src family protein tyrosine kinases and cellular signal transduction pathways. *Curr. Opin. Cell Biol.* 7:176–182.
18. Fantus, G., S. Kadota, G. Deragon, B. Foster, and B.I. Posner. 1989. Pervanadate [peroxide(s) of vanadate] mimics insulin action in rat adipocytes via activation of the insulin receptor tyrosine kinase. *Biochemistry.* 28:8864–8871.
19. Ferro-Novick, S., and R. Jahn. 1994. Vesicle fusion from yeast to man. *Nature (Lond.).* 370:191–193.
20. Gazit, A., P. Yaish, C. Gilon, and A. Levitzki. 1989. Tyrphostins I: synthesis and biological activity of protein tyrosine kinase inhibitors. *J. Med. Chem.* 32:2344–2352.
21. Gordon, J.A. 1991. Use of vanadate as protein-phosphotyrosine phosphatase inhibitor. *Methods Enzymol.* 201:477–482.
22. Green, R., and D. Shields. 1984. Somatostatin discriminates between the intracellular pathways of secretory and membrane proteins. *J. Cell Biol.* 99:97–104.
23. Hay, J.C., and T.F.J. Martin. 1993. Phosphatidylinositol transfer protein required for ATP-dependent priming of Ca^{2+}-activated secretion. *Nature (Lond.).* 366:572–575.
24. Hay, J.C., P.L. Fisette, G.H. Jenkins, K. Fukami, T. Takenawa, R.A. Anderson, and T.F.J. Martin. 1995. ATP-dependent inositide phosphorylation required for Ca^{2+}-activated secretion. *Nature (Lond.).* 374:173–177.
25. Heffetz, D., I. Bushkin, R. Dror, and Y. Zick. 1990. The insulinomimetic agents H_2O_2 and vanadate stimulate protein tyrosine phosphorylation in intact cells. *J. Biol. Chem.* 265:2896–2902.
26. Huber, L.A., S. Pimplikar, R.G. Parton, H. Virta, M. Zerial, and K. Simons. 1993. Rab8, a small GTPase involved in vesicular traffic between the TGN and the basolateral plasma membrane. *J. Cell Biol.* 123:35–45.
27. Jena, B.P., P.J. Padfield, T.S. Ingebritsen, and J.D. Jamieson. 1991. Protein tyrosine phosphatase stimulates Ca^{2+}-dependent amylase secretion from pancreatic acini. *J. Biol. Chem.* 266:17744–17746.
28. Jiang, H., Z. Lu, J.-Q. Luo, A. Wolfman, and D.A. Foster. 1995. Ras mediates the activation of phospholipase D by v-Src. *J. Biol. Chem.* 270:6006–6009.
29. Jiang, H., J.-Q. Luo, T. Urano, P. Frankel, Z. Lu, D.A. Foster, and L.A. Feig. 1995. Involvement of Ral GTPase in v-Src-induced phospholipase D activation. *Nature (Lond.).* 378:409–412.
30. Jones, S.M., J.R. Crosby, J. Salamero, and K.E. Howell. 1993. A cytosolic complex of p62 and rab6 associates with TGN38/41 and is involved in budding of exocytic vesicles from the *trans*-Golgi network. *J. Cell Biol.* 122:775–788.
31. Ktistakis, N.T., H.A. Brown, P.C. Sternweis, and M.G. Roth. 1995. Phospholipase D is present on Golgi-enriched membranes and its activation by ADP ribosylation factor is sensitive to brefeldin A. *Proc. Natl. Acad. Sci. USA.* 92:4952–4956.
32. Ktistakis, N.T., H.A. Brown, M.G. Waters, P.C. Sternweis, and M.G. Roth. 1996. Evidence that phospholipase D mediates ADP ribosylation factor–dependent formation of Golgi coated vesicles. *J. Cell Biol.* 134:295–306.
33. Lamaze, C., and S.L. Schmid. 1995. Recruitment of epidermal growth factor receptors into coated pits requires their activated tyrosine kinase. *J. Cell Biol.* 129:47–54.
34. Levitzki, A., and A. Gazit. 1995. Tyrosine kinase inhibition: an approach to drug development. *Science (Wash. DC).* 267:1782–1788.
35. Leyte, A., F.A. Barr, R.H. Kehlenbach, and W.B. Huttner. 1992. Multiple trimeric G-proteins on the trans-Golgi network exert stimulatory and inhibitory effects on secretory vesicle formation. *EMBO (Eur. Mol. Biol. Organ.) J.*11:4795–4804.
36. Li, R.Y., F. Gaits, A. Rageb, J.M. Rageb-Thomas, and H. Chap. 1995. Tyrosine phosphorylation of an SH2-containing protein tyrosine phosphatase is coupled to platelet thrombin receptor via pertussis toxin-sensitive heterotrimeric G-protein. *EMBO (Eur. Mol. Biol. Organ.) J.*14: 2519–2526.
37. Ling, W.L.W., and D. Shields. 1996. Formation of secretory vesicles in permeabilized cells: a salt extract from yeast membranes promotes budding of nascent secretory vesicles from the trans-Golgi network of endocrine cells. *Biochem. J.* 314:723–726.
38. Liscovitch, M., and L.C. Cantley. 1995. Signal transduction and membrane traffic: the PITP/phosphoinositide connection. *Cell.* 81:659–662.
39. Malarkey, K., C.M. Belham, A. Paul, A. Graham, A. McLees, P.H. Scott, and R. Plevin. 1995. The regulation of tyrosine kinase signalling pathways by growth factor and G-protein-coupled receptors. *Biochem. J.* 309: 361–375.
40. Narula, N., I. McMorrow, G. Plopper, J. Doherty, K.S. Matlin, B. Burke, and J.L. Stow. 1992. Identification of a 200-kD, brefeldin-sensitive protein on Golgi membranes. *J. Cell Biol.* 117:27–38.
41. Nuoffer, C., and W.E. Balch. 1994. GTPases: multifunctional molecular switches regulating vesicular traffic. *Annu. Rev. Biochem.* 63:949–990.
42. Ohashi, M., and W.B. Huttner. 1994. An elevation of cytosolic protein phosphorylation modulates trimeric G-protein regulation of secretory vesicle formation from the *trans*-Golgi network. *J. Biol. Chem.* 269: 24897–24905.
43. Ohashi, M., K. Jan de Vries, R. Frank, G. Snoek, V. Bankaitis, K. Wirtz, and W. Huttner. 1995. A role for phosphatidylinositol transfer protein in secretory vesicle formation. *Nature (Lond.).* 377:544–547.
44. Pfeffer, S.R. 1994. Rab GTPases: master regulators of membrane trafficking. *Curr. Opin. Cell Biol.* 6:522–526.
45. Pimplikar, S.W., and K. Simons. 1993. Regulation of apical transport in epithelial cells by a G_s class of heterotrimeric G protein. *Nature (Lond.).* 362:456–458.
46. Pimplikar, S.W., and K. Simons. 1994. Activators of protein kinase A stimulate apical but not basolateral transport in epithelial Madin-Darby canine kidney cells. *J. Biol. Chem.* 269:19054–19059.
47. Posner, B.I., R. Faure, J.W. Burgess, A.P. Bevan, D. Lachance, G. Zhang-Sun, I.G. Fantus, J.B. Ng, D.A. Hall, B.S. Lum, and A. Shaver. 1994. Peroxovanadium compounds. *J. Biol. Chem.* 269:4596–4604.
48. Pryde, J.G. 1994. A group of integral membrane proteins of the rat liver Golgi contains a conserved protein of 100 kDa. *J. Cell Sci.* 107:3425–3436.
49. Pumiglia, K.M., L.-F. Lau, C.-K. Huang, S. Burroughs, and M.B. Feinstein. 1992. Activation of signal transduction in platelets by the tyrosine phosphatase inhibitor pervanadate (vanadyl hydroperoxide). *Biochem. J.* 286: 441–449.
50. Randazzo, P.A., T. Terui, S. Sturch, and R.A. Kahn. 1994. The amino terminus of ADP-ribosylation factor (ARF) 1 is essential for interaction with G_s and ARF GTPase-activating protein. *J. Biol. Chem.* 269:29490–29494.
51. Rothman, J.E. 1994. Mechanisms of intracellular protein transport. *Nature (Lond.).* 372:55–63.
52. Santini, F., and J.H. Keen. 1996. Endocytosis of activated receptors and clathrin-coated pit formation: deciphering the chicken or egg relationship. *J. Cell Biol.* 132:1025–1036.
53. Slack, B.E., J. Breu, M.A. Petryniak, K. Srivastava, and R.J. Wurtman. 1995. Tyrosine phosphorylation-dependent stimulation of amyloid precursor protein secretion by the m3 muscarinic acetylcholine receptor. *J. Biol. Chem.* 270:8337–8344.
54. Stack, J.H., B. Horazdovsky, and S.D. Emr. 1995. Receptor-mediated protein sorting to the vacuole in yeast: roles for a protein kinase, a lipid kinase and GTP-binding proteins. *Annu. Rev. Cell Dev. Biol.* 11:1–33.
55. Stanners, J., P.S. Kabouridis, K.L. McGuire, and C.D. Tsoukas. 1995. Interaction between G proteins and tyrosine kinases upon T cell receptor-CD3-mediated signalling. *J. Biol. Chem.* 270:30635–30642.
56. Stoller, T.J., and D. Shields. 1988. Retrovirus-mediated expression of preprosomatostatin: posttranslational processing, intracellular storage, and secretion in GH3 Pituitary Cells. *J. Cell Biol.* 107:2087–2095.
57. Streuli, M. 1996. Protein tyrosine phosphatases in signaling. *Curr. Opin. Cell Biol.* 8:182–188.
58. Sun, H., and N.K. Tonks. 1994. The coordinated action of protein tyrosine phosphatases and kinases in cell signalling. *Trends Biochem. Sci.* 19:480–485.
59. Trudel, S., M.R. Paquet, and S. Grinstein. 1991. Mechanism of vanadate-induced activation of tyrosine phosphorylation and of the respiratory burst in HL60 cells. *Biochem. J.* 276:611–619.
60. Van der Geer, P., and T. Hunter. 1994. Receptor protein-tyrosine kinases and their signal transduction pathways. *Annu. Rev. Cell Biol.* 10:251–337.
61. Walton, K.M. and J.E. Dixon. 1993. Protein tyrosine phosphatases. *Annu. Rev. Biochem.* 62:101–120.
62. Xu, H., and D. Shields. 1993. Prohormone processing in the *trans*-Golgi network: endoproteolytic cleavage of prosomatostatin and formation of nascent secretory vesicles in permeabilized cells. *J. Cell Biol.* 122:1169–1184.
63. Xu, H., P. Greengard, and S. Gandy. 1995. Regulated formation of Golgi secretory vesicles containing Alzheimer β-amyloid precursor protein. *J. Biol. Chem.* 270:23243–23245.